Proceedings of IMECE2007
2007 ASME International Mechanical Engineering Congress and Exposition
November 11-15, 2007, Seattle, Washington, USA

IMECE2007-43687

AN EXPERIMENT TO DETERMINE THE ACCURACY OF SQUEEZE-FILM DAMPING MODELS IN THE FREE-MOLECULE REGIME

Hartono Sumali
Sandia National Laboratories
MS 1070, PO Box 5800
Albuquerque, NM 87185
hsumali@sandia.gov

ABSTRACT

Relying on differing assumptions, published models for predicting squeeze-film damping (SFD) give widely different results in the free-molecule regime, where the distance traveled by gas molecules between collisions in free space is much larger than the thickness of the film. The work presented here provides experimental data for validating SFD models. The test device was an almost rectangular MEMS oscillating plate supported by beam springs. The structure was base-excited, and the velocities of the suspended plate and of the substrate were measured with a laser Doppler vibrometer and a microscope. Experimental modal analysis processed the velocity to give the damping ratio. The test structures were contained in a vacuum chamber with air pressures controlled to provide a five-order-of-magnitude range of Knudsen numbers. The damping coefficients from the measurements were compared with predictions from various published models. The resulting knowledge of damping as a function of Knudsen number is useful in designing many structures such as MEMS oscillators, sensors and switches.

NOMENCLATURE

a	plate width, m	R	universal gas constant,
b	plate length, m	T	temperature, K
c	damping coefficient, Ns/m	t	time, s
c_s	solid damping coefficient, Ns/m	z	gap displacement
e_0	amplitude, m	z_p	plate displacement
h	mean gap height, m	z_b	base displacement
h_{plate}	plate thickness, m	μ	viscosity, Pa s
j	$\sqrt{-1}$	ρ	gas density, kg/m^3
k	spring stiffness, N/m	ρ_{plate}	plate density, kg/m^3
k_B	Boltzmann's constant		
k_s	structural spring stiffness, N/m	λ	mean free path, m
m	plate mass, kg	σ	squeeze number, nd
m_m	molecular mass, kg/mol	ω	frequency, rad/s
P	ambient pressure, Pa	ω_n	natural frequency, rad/s
p	pressure at (x,y), Pa	ζ	modal damping ratio, nd

nd = non-dimensional.

1 INTRODUCTION

Oscillating structures at the micron and smaller scales have played an important and increasing role in the last two decades because of such applications as the atomic force microscope, resonant sensors, and MEMS oscillators. Because of the high surface-to-mass ratios, dynamic motions of small structures are affected tremendously by fluid damping. For most planar MEMS structures, the dominant fluid damping is squeeze-film damping (SFD), where fluid is squeezed in and out of a gap between the moving structure and the substrate (Fig. 2).

Continuum-based models assume that the gas is a continuum, meaning that gradient of pressure is continuous throughout the gas. Continuum-based squeeze film damping models are based on the linearized Reynolds equation (Blech, 1983).

$$\frac{Ph^2}{12\mu}\nabla^2\left(\frac{p}{P}\right)-\frac{\partial}{\partial t}\left(\frac{p}{P}\right)=\frac{\partial}{\partial t}\left(\frac{z}{h}\right), \qquad (1)$$

where x and y denotes coordinate axes, and z is the plate displacement in Eq. (1). $z = 0$ when the distance between the plate and the base is h.

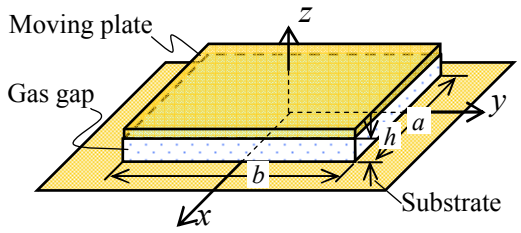

Figure 1: Squeezed gas film between a substrate and a moving plate.

Continuum-based models may break down when the distance traveled by gas molecules between collisions in free space is much larger than the thickness of the gap (Fig. 2). In that rarefied or free-molecule regime, gradients are not continuous, or do not even exist. Therefore, some researchers argue that continuum models should not be used in the free-

molecule regime (Bhiladvala and Wang, 2004). The regime of gas damping is determined by the Knudsen number, which is the molecular mean-free-path length divided by the thickness of the gap. The free path length is illustrated in Fig. 1 as the distance traveled by a particle from one collision to the next. The mean free path is

$$\lambda = \frac{\mu}{P}\sqrt{\frac{2RT}{m_m}} \tag{2}$$

The Knudsen number is

$$K_s = 1.016\ \lambda/h. \tag{3}$$

Schaaf and Chambre (1961) define the free-molecule regime as $K_s > 10$. Knudsen numbers are high when the gap is very small, as typical of micro- and nano-scale structures. In experiments, high Knudsen numbers can also be achieved by lowering the gas pressure.

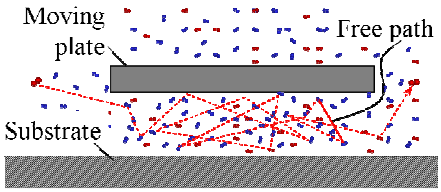

Figure 2: Gas particles between a substrate and a moving plate.

Lacking experimental data, published models for predicting SFD are based on varying assumptions. Those models give widely different results especially in the free-molecule regime. The work presented here attempts to provide experimental data for comparing the existing SFD models, helping in making decision on which model(s) to use.

2. GAS DAMPING MODELS

2.1 Non-Gradient-Based Models

For lack of a better concise term, this text will use the term *non-gradient-based models* to refer to models that are not based on continuum equations like Eq. (1). The non-gradient-based models discussed here are based on the reasoning that gas damping forces on solid structures are caused by the collisions of the gas molecules impinging on the structure's surfaces. When bouncing on a plate, gas particles impart momentum change. A statistical average of the momentum change from all the particles bouncing on the plate results in pressure. If a plate moves in the gas, the leading face of the plate will receive a higher pressure than the trailing face. The difference in pressures creates the damping force. The non-gradient-based models in the next few paragraphs have been compared to damping measured on a micro scale silicon beam by Zook et al (1992) (henceforth *Zook's data*). The comparisons will be shown in this section after a brief summary of the models. The models predict the damping factor, which is

$$c = -F_{damping} / \dot{z}_{plate} \tag{4}$$

where $F_{damping}$ is the force on the plate due to gas damping, and $\dot{z}_{plate}$ is the velocity of the plate.

Christian (1966) proposed that

$$c^{Christian} = 4\sqrt{\frac{2m}{\pi k_B T}}Ap \tag{5}$$

where

Newell (1968) used Christian's model to derive gas damping coefficient

$$c^{Newell} = \sqrt{\frac{2m}{\pi k_B T}}\frac{p}{\rho b f_r} \tag{6}$$

Newell's model was used by Zook et al (1992), who provided experimental data against which other researchers have compared their gas damping models.

Kádár et al (1996) proposed an improvement to Christian's model by replacing its Maxwell-Boltzman gas molecule velocity distribution with the Maxwellian stream distribution, resulting in

$$c^{Kádár} = \pi\, c_{Chrstian} \tag{6}$$

Li et al (1999) improved on Kádár et al's model by correcting the velocity of the moving structure relative to the fluid, resulting in

$$c_{Li} = \frac{1.5\pi}{1+\frac{M}{3R_0T}u^2}c_{Christian} \tag{7}$$

In comparing their models to Zook's data, the authors of the above three models assumed that the structure in Zook et al's experiment was moving in free space, and there was no gap or substrate to create a squeezed film. Kádár et al argues that, in the rarefied gas regime, squeeze film damping is the same as free-space damping. However, Bao et al (2002) pointed out that the geometry of the gap should have been included in the models since the gas was squeezed between the moving structure and the substrate. Bao et al's correction resulted in

$$c_{Bao} = \frac{L_{circumference}/h}{16\pi}c_{Christian}, \tag{8}$$

where, for a rectangular plate with a width a and length b,

$$L_{circumference} = 2(a+b). \tag{9}$$

The above models were not derived from gradient-based theory like the Reynolds equation. Their derivation is based on reasoning of the averaged effect of gas particles colliding on the structure. However, they are not based on actual molecular dynamics either. A model that is truly based on molecular dynamics was developed by Hutcherson and Ye (2004), who developed a molecular dynamics code that simulated the motion of a large number of molecules in the squeezed gas film. Using Bao's assumptions, Hutcherson and Ye's

simulation reproduced Bao's result. Subsequently, Hutcherson and Ye employed an improved relationship between the particle velocity and the number of collisions, and showed that the resulting damping factor for Zook's beam was 2.233 times higher than Bao's calculation.

Except for Christian's model, the attempt to validate the above models was to compare them to Zook's data. Zook et al performed the measurement on a micro-beam of the following properties: length b = 200μm, width a = 40μm, and gap size h = 1.1μm. Using those parameters, the models are used here to calculate the quality factor Q, which is then translated into the damping ratio ζ defined here as

$$\zeta = 0.5/Q \tag{10}$$

The resulting damping ratios are plotted against pressure in Fig. 3. Hutcherson and Ye's molecular dynamic simulation results are directly from their publication. Zook's measurement result plotted on the same graph shows that each model improvement brings the damping ratios closer to the measured damping ratio.

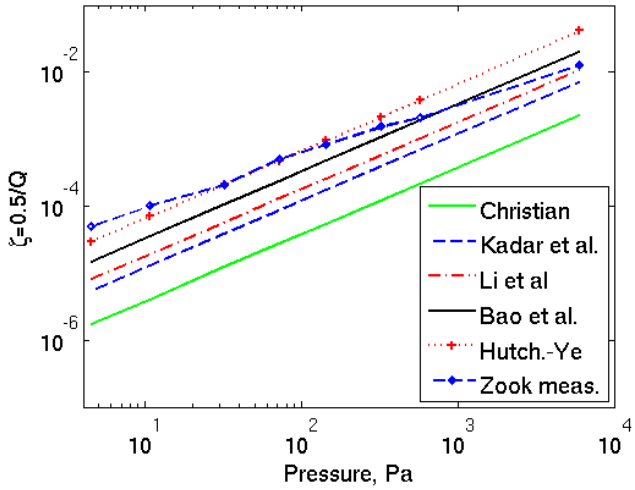

Figure 3: Damping ratio calculations from published particle-based models attempting to match published measured data.

From Fig. 3, it is apparent that the most improved model, i.e. Hutcherson and Ye's, is the closest to the measured data in the rarefied regime. However, Bao et al's model is closer to the measured data at 1000Pa or higher. In fact, at 10^4 Pa Hutcherson and Ye's damping is almost an order of magnitude higher than Zook's data. Each model improvement resulted in a factor, which is a vertical shift of the damping-versus-pressure curve on the log-log scale. All of the model results have the same slope. On the other hand, Zook et al's measured damping curve has a slope that is significantly different from the models' slope. This difference calls for a closer scrutiny of the assumptions used in deriving the models, especially of whether those assumptions agree with the conditions under which Zook et al's damping data were obtained. The comparisons below is limited to region II in Zook et al, in which the gas is rarefied, but damping in the solid ("intrinsic damping") is negligible compared to gas damping.

Zook et al mentioned that a source of discrepancy between Newell's damping calculation and Zook's data was that the geometries of the air space were quite different. The calculation assumed free or open space. The measurement was done on a beam sandwiched between two squeezed air film, one beneath the beam and another on top of the beam. Squeeze-film damping can be much higher than free space gas damping especially if the squeezed gas film is very thin.

The second source of discrepancy was the structural boundary conditions of the beam. Table 1 has sketches of boundary conditions used in deriving the models above versus the boundary conditions of the structures used in obtaining data for validating the models. Zook et al used Christian/Newell model for a cantilever (clamped-free) beam. Yet they showed that their test structure was a clamped-clamped beam. In fact, their finite element simulation with the clamped-clamped boundary conditions resulted in natural frequencies that agreed very well with their measured natural frequency. The structural velocity distribution of the cantilever is very different from that of a clamped-clamped beam. For example, the right end of Newell's cantilever has the highest velocity of all points along the beam. On the other hand, the right end of Zook et al's beam has zero velocity. Gas damping calculation from Christian/Newell's model probably should not be compared directly to Zook's data.

Kádár et al and Li et al derived their gas damping model for a rigid beam pivoting about its center with some torsional spring. The ends of the beam had the highest structure velocity. Yet they compared the calculation directly to Zook's measured beam, where the ends of the beam had zero velocity.

Bao et al and Hutcherson and Ye developed their models for the case where the gas damping is caused by an air film squeezed between the moving plate and the substrate. Zook et al showed that the gas damping on their test device was indeed caused by squeezed films. But in fact there were two squeezed film in their test device because, in addition to the substrate, the device also had a lid close to the beam. Another source of discrepancy between the models and Zook's data was the fact that the test structure was a flexible beam. Bao et al and Hutcherson and Ye's models assume a rigid beam moving up and down. In the models the ends of the beam move at the same velocity as the center of the beam. In Zook's device, the ends of the beam were clamped and had zero velocity.

Table 1 and Fig. 4 lead to the following conclusion from the above literature study: models that do not use the structural velocity distribution correctly will not predict gas damping correctly.

Table 1: Structures assumed in deriving gas damping equations (middle column) versus structures measured for validation data (right column).

Reference	Structure assumed in model	Structure used in comparison measurement
Christian 1996		Nothing conclusive
Newell 1968	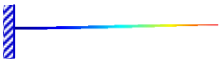	None
Zook et al. 1992	Newell (see above)	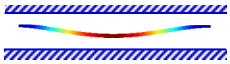
Kádár et al. 1996		Zook et al. (see above)
Li et al. 1999	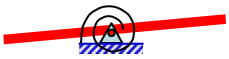	Zook et al. (see above)
Bao et al. 2002		Zook et al. (see above)
Hutcherson and Ye 2004		Zook et al. (see above)

Modeling the structural velocity distribution of a plate vibrating with squeeze film damping is by no means a trivial task. Nayfeh and Younis (2003) developed a model that does that task elegantly for a flexible clamped-clamped beam like the beam in Zook et al's experiment. Their squeeze film damping calculation agrees well with experimental data published by Legtenberg and Tilmans (1994) from atmospheric pressure down to five orders of magnitudes lower. Agreement with the experimental data at such low pressures shows that their model is quite accurate in the free-molecule regime.

2.2 Continuum Models

It must be pointed out that Nayfeh and Younis's model was based on the continuum Reynolds equation without any molecular dynamics. The lesson learned from the comparison among models so far is that the continuum Reynolds equation may well be more accurate than the non-gradient-based models discussed so far -- in the non-continuum regime. Reynolds-equation-based squeeze film damping models are worth considering for prediction of damping in the free-molecule regime. Besides the indication of accuracy mentioned above, the reasons for using the continuum models include the following. Continuum models have been developed and established longer than molecular-based models. The constitutive equations used for developing continuum models have long been proven.

Except Christian and Newell who predated Zook et al, all the researchers in Table 1 used Zook's data even though their theoretical derivation was based on very different conditions. The reason was that very few publications presented experimental data for rarefied gas damping better than Zook's data. Consequently, none of the publications show in Table 1 shows a model and experimental data that are both based on a common structure and boundary conditions. An attempt to validate a model with an experiment based on different conditions than the model is not likely to be meaningful. On the other hand, for continuum-based models experimental data are available from tests under conditions that match the model assumptions. This is another important reason to consider continuum models for predicting SFD in the free-molecule regime. Table 2 lists the references that present such models and references that present experimental data correctly corresponding to the models. This paper will discuss only the case of a rigid rectangular plate moving up and down, squeezing a gas film between the plate and the substrate.

Table 2: A few squeeze film damping theories that have been compared with experiments on a micro structure with boundary conditions consistent with the theory.

	Rigid structure 	Flexible Structure 
Theory	Blech 1983, Veijola 2004, Gallis and Torczynski 2004.	Nayfeh and Younis 2003
Experiment	Andrews et al. 1992, Veijola 2004, Sumali and Epp 2006.	Zook et al 1992, Legtenberg and Tilmans 1994, Cheng and Fang 2005.

Yet another reason for using Reynolds-equation-based models is that the Reynolds equation facilitates the calculation and the use of correct pressure distribution throughout the plate due to SFD. To illustrate that statement, Fig. 4 shows a model of what was likely to have happened in Zook et al's experiment with the clamped-clamped beam. Fig 4.a is a cartoon of the deflected beam positioned between the substrate beneath and the lid above. In deflecting, the beam squeezes the air films, one film between the beam and the lid, and another film between the beam and the substrate. For this illustration, a finite element model was developed using the commercial package COMSOL™, using Zook et al's dimensions and the squeeze-film damping model in the MEMS module. Figure 4.b shows that the pressure due to SFD varies not only along the beam, but also across the width of the beam even though the deflection of the beam is not a function of position across the width. Reynolds-equation-based models facilitate correct pressure distribution throughout the plate due to SFD, unlike the models in Table 1. (Finite element methods and models for calculating SFD will not be discussed further in this paper, since the paper's objective is to compare reduced-order models.)

The Reynolds-equation-based models discussed in this paper assume:

1. Rigid plate;
2. Small gap $h/a<<1$;
3. Small displacement $e_0/h<<1$;
4. Small pressure variation $p/P<<1$;

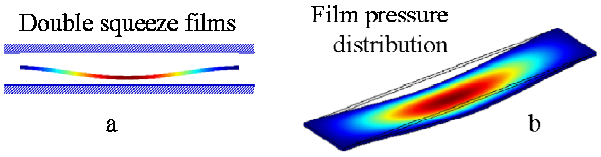

Figure 4: a)Damping from double-squeezed films; b)Non-uniform distribution of pressure throughout the beam.

2.2.1 Blech's Model

In addition to the four assumptions above, Blech's model assumes:

5. Isothermal process;
6. The pressure right outside the plate edges = P (trivial boundary condition);
7. Small molecular mean free path
8. No inertial effects of gas moving in and out of the gap.

The damping coefficient as a function of the plate oscillation frequency is

$$c^{Blech}(\omega)=\frac{768}{\pi^6}\frac{a^3 b}{h^3}\mu\sum_{m,n\ \text{odd}}\frac{m^2+n^2(a/b)^2}{m^2n^2\left[m^2+n^2(a/b)^2\right]^2+\sigma^2/\pi^4}, \quad (11)$$

where frequency and pressure are combined into the *squeeze number*

$$\sigma=12\mu\left(\frac{a}{h}\right)^2\left(\frac{\omega}{P}\right) \quad (12)$$

Assumptions 7 and 8 above mean that Blech's model is not to be used for predicting SFD in the rarefied gas regime. The model was developed mainly for liquid films. It is included here because it is important historically and in many practical SFD calculations, and its limit is an extremely simple model, discussed next.

2.2.2 Andrews et al's Model

For low squeeze numbers, Blech's model reduces to [2]

$$c^{Andrews}=0.42\frac{a^2b^2\mu}{h^3}, \quad (13)$$

henceforth referred to as Andrews et al's model. Despite its extreme simplicity, Andrews et al's model will be shown later to be quite accurate in the low Knudsen number regime.

2.2.3 Veijola's Model

Veijola (2004) did away with Blech's assumptions 6 and 7 above. Perhaps the most significant feature of the resulting model is the replacement of the trivial boundary conditions with a boundary condition that gives a much more accurate transition from the pressure in the gas film under the footprint of the plate into the ambient pressure away from the plate. This is a major improvement over Blech's and other models, that assume that the pressure under the perimeter of the plate is the ambient pressure (trivial boundary condition).

To use Veijola's model, first, calculate the modified Reynolds number

$$R_e=\rho h^2\omega/\mu. \quad (14)$$

Then calculate a complex frequency variable

$$q=\sqrt{j\omega\rho/\mu}/h \quad (15)$$

Veijola's SFD model also takes into account the inertia of the squeezed gas film. A frequency-dependent coefficient that accounts for the effect of inertia on the flow of gas in and out of the gap is

$$Q_{\text{pr}}=\frac{12\mu}{j\omega\rho h^3 q}\left[\frac{qh-\left(2-q^2 1.016\lambda h\right)\tanh(qh/2)}{1+1.016\lambda q\tanh(qh/2)}\right], \quad (16)$$

The above coefficient is used to modify Reynolds equation. The solution for a rectangular plate is a series summation over odd indices m and n containing the terms

$$G_{mn}=\frac{\pi^6 h^3(mn)^2}{768\mu ab}\left(\frac{m^2}{a^2}+\frac{n^2}{b^2}\right) \quad (17)$$

and

$$C_{mn}=\frac{\pi^4 h(mn)^2}{64abn_\gamma P}. \quad (18)$$

Finally, the gas damping coefficient is

$$c^{Viej}(\omega)=\text{Re}\left[\sum_{m=1,3,\ldots}^{M}\sum_{n=1,3,\ldots}^{N}\frac{1}{Q_{\text{pr}}G_{mn}+j\omega C_{mn}}\right]. \quad (19)$$

In the above equation, Re[] means "the real part".

2.2.4 Gallis and Torczynski's Model

Gallis and Torczynski (2004) developed a truly molecular-dynamics-based model by Direct Simulation Monte Carlo method for SFD on a rigid beam. Their model takes advantage of both Reynolds equation and molecular dynamics. It is free from many assumptions that limited earlier models. In particular, it is free from trivial boundary conditions. Furthermore, Gallis and Torczynski adapted that model with a continuum-based shape factor derived for a plate. The result is summarized in Sumali et al (2007).

3. NEW TEST STRUCTURE AND ITS MODEL

Figure 3 shows that it would be very difficult to explain the slope in Zook's data perfectly with any of the model discussed

here. A new set of data will be very useful. The test structure discussed in this paper can be modeled as a rigid rectangular plate supported by springs as shown in Fig. 5. A gas layer is squeezed between the plate and the stationary base. (Details of the structure can be found in the Experiment section later.) Figure 5 shows the plate suspended by a structural spring k_s and structural damping dashpot c_s. To excite oscillations, the base is vibrated with a displacement $Z_b(\omega)$, where ω denotes radian frequency. The displacement response of the plate is $Z_p(\omega)$. The difference between $Z_p(\omega)$ and $Z_b(\omega)$ is here referred to as the *gap squeeze*

$$z = z_p - z_b, \tag{20}$$

which expands and squeezes the air gap between the base and the plate, resulting in squeezed-gas force. (Capital letters denote the Fourier transform of the corresponding variable in lower case letters.)

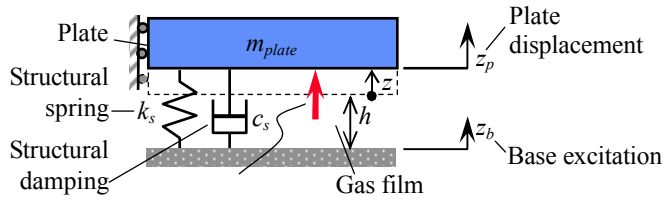

Figure 5: Model of oscillating plate showing squeeze-film force.

The acceleration of plate is

$$m\ddot{z}_p = kz + c\dot{z}, \tag{21}$$

where the total damping coefficient is

$$c = c_s + c^{gas}. \tag{22}$$

The total damping coefficient c will be obtained from the experiments. The structural damping coefficient c must be subtracted from the total damping coefficient to obtain the gas damping coefficient c^{gas} , which will later compared with the various gas damping models discussed in the previous sections.

The experiment measures the plate displacement z_p and the base excitation displacement z_b. Therefore, the transmissibility from base displacement to plate displacement,

$$H_{meas}(\omega) = Z_p(\omega)/Z_b(\omega), \tag{23}$$

is obtained from the measurement. The above measured transmissibility can be used to calculate the frequency response function from the base displacement to the gap squeeze, which can be shown to be

$$H(\omega) = \frac{Z(\omega)}{Z_b(\omega)} = \frac{\omega^2}{-\omega^2 + j\omega 2\zeta\omega_n + \omega_n^2}. \tag{24}$$

whereζ is the damping ratio defined as

$$\zeta = c/(2m_{eff}\omega_n), \tag{25}$$

and ω_n is the natural frequency which is

$$\omega_1 = \sqrt{k/m_{eff}}\ . \tag{26}$$

The effective mass m_{eff} is the mass of the plate augmented by a portion of the mass of the springs because the springs oscillate with the plate. A lumped-parameter system equivalent to the mass-springs structure can be derived with the Rayleigh method (Blevins, 1995):

$$m_{eff} = m_{plate} + 4\times 0.37 m_{spring}\ . \tag{27}$$

The factor 4 is inserted because the structure has four springs. The plate mass m_{plate} is estimated from the measured plate dimensions and a mass density of 19300 kg/m^3 for gold. It is assumed that the thickness is uniform throughout the structure. From Eq. (21) and (23), it can be shown that

$$H(\omega) = H_{meas}(\omega) - 1. \tag{28}$$

Curve fitting of $H(\omega)$ into the form in Eq. (24) will give the natural frequency ω_n and damping ratio ζ. To obtain the gas damping ratio ζ^{gas}, the structural damping ratio must be subtracted from the total damping ratio ζ. Following Eq. (22),

$$\zeta^{gas} = \zeta - \zeta_s, \tag{29}$$

where ζ_s is the structural damping ratio. Thus, the gas damping ratio ζ^{gas} can be obtained from the measured transmissibility, provided that the structural damping ratio ζ_s is known. (A method to obtain the structural damping ratio will be presented later.) The gas damping coefficient c^{model} from the models discussed earlier can be converted into gas damping ratios ζ^{model} using E.q (25), and finally compared with the measured gas damping ratio ζ^{gas}.

4. EXPERIMENT

Figure 6 shows the test structure, which consisted of a plate suspended by four folded-beam springs. One end of each spring supports the plate, and the other end is anchored to the substrate. The structures were made of electro-deposited gold. The design width of the plate was a = 155.6 μm.

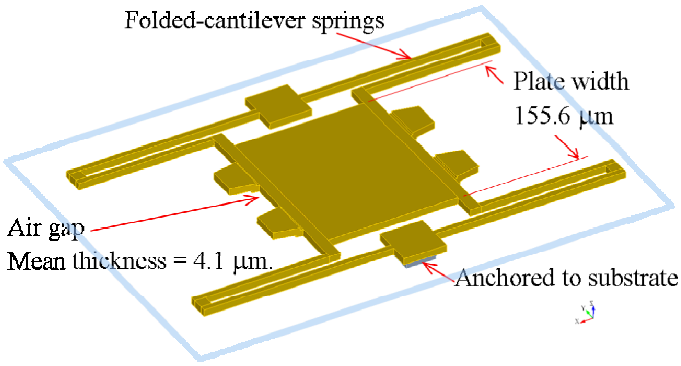

Figure 6: Test structure.

Designed originally as MEMS switches, the test structures had a plate that was not rectangular as modeled in the previous sections. The four trapezoidal tabs on the ends of the plate were designed to carry contact dimples for conducting electrical transmission. In applying the analytical models described above for rectangular plates, the needed length b is estimated by equating the area of the plate including the four trapezoidal tabs to ab, as shown in Fig. 7.

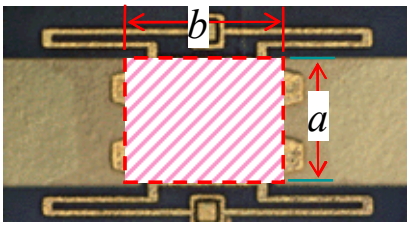

Figure 7: Equivalent length b = Area of plate including tabs divided by width of plate a.

The experimental setup can be summarized as follows. A piezoelectric transducer shakes the substrate with random vertical displacement. As a result, the plate oscillates vertically, expanding and squeezing the air layer between the plate and the substrate. The suspension springs flex and provide a restoring force to sustain the oscillation. A laser Doppler vibrometer (LDV) with a microscope measured the velocities at one point on the substrate (the "base"), and 21 points all over the plate and the springs. All data were obtained under small excitations where linear responses were verified. The spot size of the laser was about 1 μm. The test structures were contained in a vacuum chamber with air pressures from atmospheric down to five orders of magnitude lower.

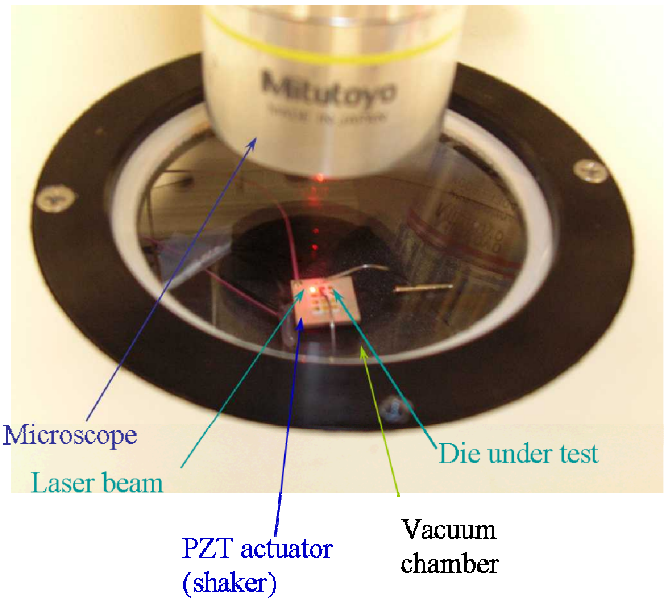

Figure 8: Test setup.

RESULT

The measured transmissibility (plate velocity divided by base velocity) is converted into the gap transmissibility using Eq. (28). A typical set of gap transmissibilities is shown in Fig. 9. Using a commercial package ME'ScopeTM, experimental modal analysis (EMA) was performed on the gap transmissibilities to determine the natural frequency and the modal damping ratio. Mode shapes were also obtained. The EMA computed three modes shown in Fig. 10. The mode of interest is the lowest-frequency mode in which the plate oscillates vertically while staying parallel to the substrate. The two higher modes will not be discussed here.

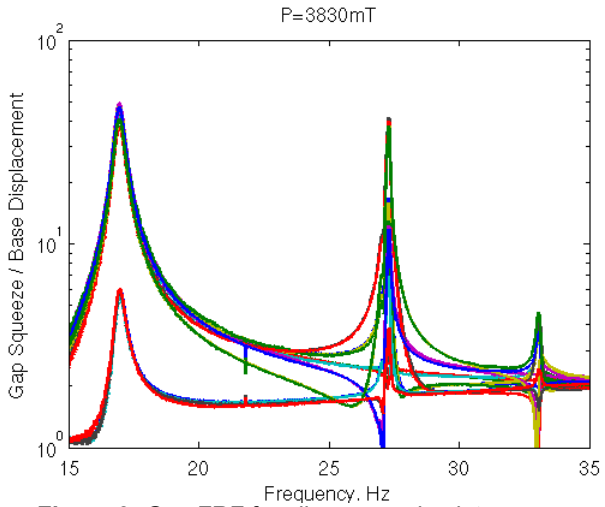

Figure 9: Gap FRF for all measured points.

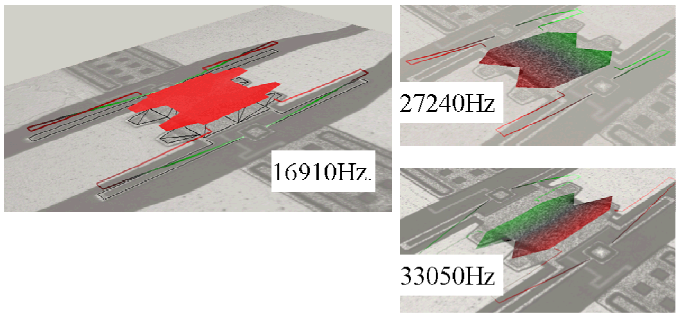

Figure 10: Measured natural frequencies and mode shapes from experimental modal analysis.

A problem in comparing the models with the measurement is the damping caused by the solid structure, referred to here as the non-squeeze-film damping (nonSFD). For damping measurements at low Knudsen numbers, nonSFD is so much lower than squeeze film damping that it can be ignored. However, at higher Knudsen numbers nonSFD dominates the damping, and therefore must be included as an important part of the comparison. As shown in Eq. (29), nonSFD must be obtained before gas damping ratios can be obtained from the measurement data. NonSFD is the damping in the solid structure in the absence of any gas, i.e., at absolute zero pressure. Because the absolute zero pressure is unattainable, nonSFD is obtained here by extrapolation. Figure 11 shows the total gas damping ratios ζ from the measurement at the seven lowest pressures. The pressure range in the graph is so narrow that the ζ -versus-pressure relationship can be assumed linear. Therefore, ζ is curve-fit as a linear function of pressure. The dashed line in Fig. 11 shows that the linear fit is justified. NonSFD, which is the structural damping ratio ζ^s, is the value of ζ at zero pressure, which is obtained as the zero-pressure intercept of the linear fit. Subsequently, ζ^{gas} is obtained by subtracting ζ^s from ζ according to Eq. (29). The resulting gas damping ratios are plotted with the + symbols in Fig. 11.

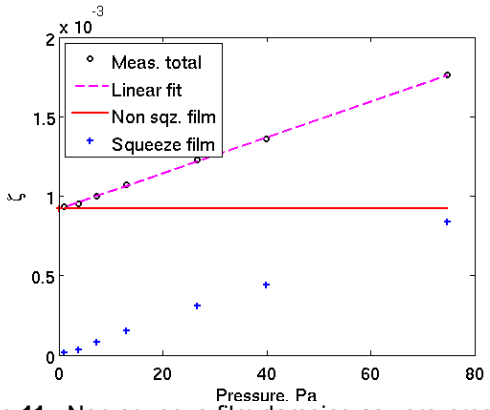

Figure 11: Non-squeeze-film damping as zero-pressure extrapolate of total measured damping.

Gas damping ratios obtained from the above process for all the pressures in the experiment are shown in Fig. 12. The plot of the measured total damping as a function of pressure has a sigmoidal shape. The zero-pressure asymptote is the non-squeeze-film damping value. At the highest pressure, the damping ratio appears to practically reach its saturation. Subtracting the non-squeeze-film damping from the total damping produces the squeeze-film damping as a function of pressure, whose plot appears to have a slope of 1 decade/decade in the low-pressure region.

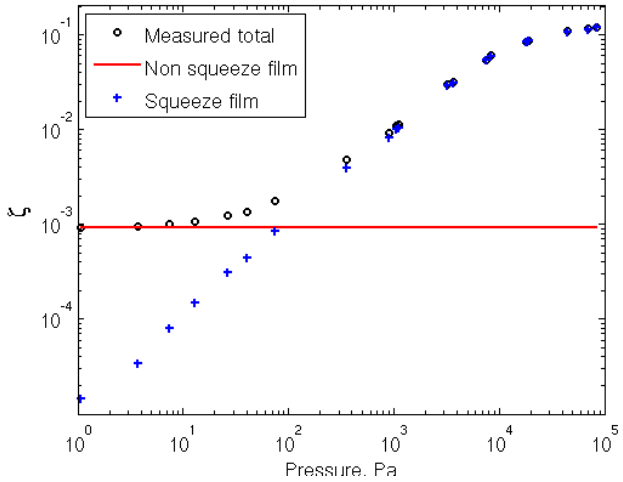

Figure 12: Measured squeeze-film damping obtained after subtracting non-squeeze-film damping from the measured total damping.

Finally, Fig. 13 show the gas damping ratio from all the models discussed above, compared with the measurement result.

CONCLUSIONS

- On rigid plates with width ~150 mm, oscillating around 4.1 mm above the substrate, squeezed air film can cause large damping.
- The non-gradient-based models developed specifically for the free-molecule regime are not necessarily more accurate than current molecular models.
- For the conditions tested here, in atmospheric air the simplest model mentioned by Andrews et al. is as good as any more sophisticated models.
- In the high squeeze number regime (low pressures or high frequencies), Veijola's model appears to match experimental data accurately.

ACKNOWLEDGMENT

The author thanks Chris Dyck for the test structures, David Epp for valuable discussions, and Dan Rader for programmatic support. This work was conducted at Sandia National Laboratories. Sandia is a multi-program laboratory operated under Sandia Corporation, a Lockheed Martin Company, for the United States Department of Energy under Contract DE-AC04-94-AL85000.

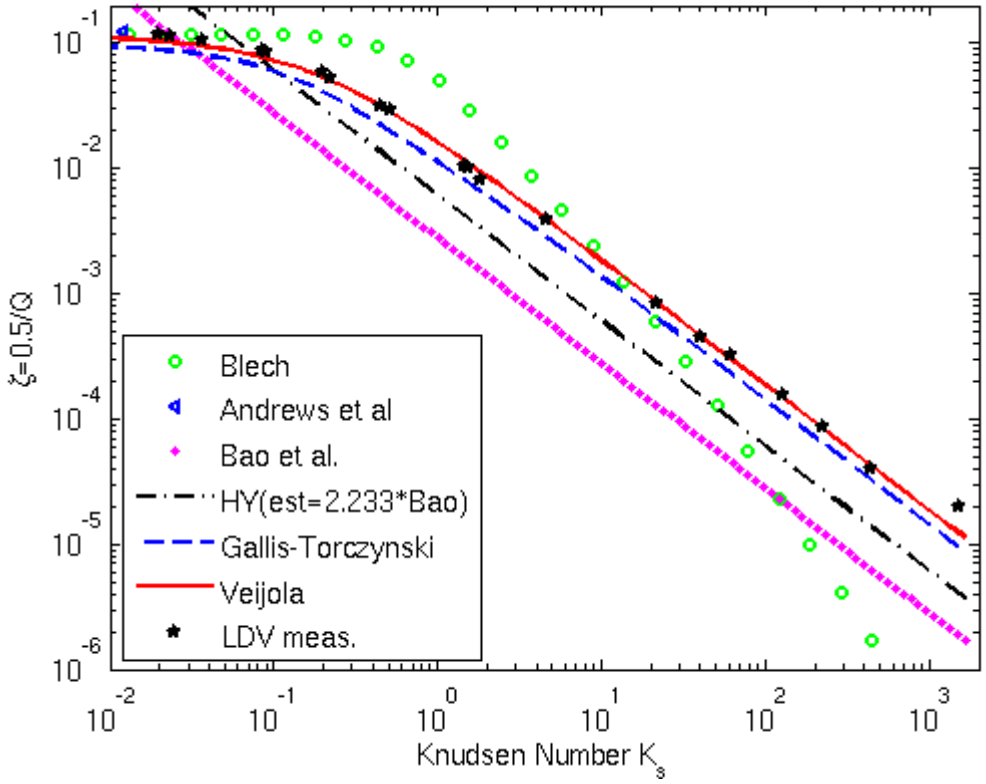

Figure 13: Comparison among gas damping models and measured gas damping as a function of Knudsen number.

REFERENCES

Andrews, M., Harris, I., Turner, G., 1993, "A comparison of squeeze-film theory with measurements on a microstructure", *Sensors and Actuators A*, **36**, p 79-87.

Bao, *M.*, Yang, H., Yin, H., and Sun, Y., 2002, "Energy Transfer model for squeeze-film air damping in low vacuum", *J. Micromech. Microeng.* **12** 341-346.

Bhiladvala, R., and Wang, J., 2004, "Effects of fluids on the *Q* factor and resonance frequency of oscillating micrometer and nanometer scale beams", *Physical Review E*, **69**, p 1-6.

Blech, J.J., 1983, "On Isothermal Squeeze Films", *Journal of Lubrication Technology*, **105**, p 615-620.

Blevins, R.D., 1995, *Formulas for Natural Frequency and Mode Shape*, Krieger, Florida, p. 159.

Cheng, C.C., and Fang, W., 2005, *Microsystem Technologies*, **11**, p 104–110

Christian, R.G., 1966, "The theory of oscillating-vane vacuum gauges", *Vacuum*, **16**, p 175.

Gallis, M.A., and Torczynski, J.R., 2004, "An Improved Reynolds-Equation Model for Gas Damping on Microbeam Motion", *Journal of Microelectromechanical Systems*, **13** (4), p 653-659.

Kádár, A., Kindt, W., Bossche, A., Mollinger, J., 1996, "Quality factor of torsional resonators in the low-pressure region", *Sensors and Actuators A*, **53** p 299-303.

Li, B., Wu, H., Zhu, C, and Liu, J., 1999, "The theoretical analysis on damping characteristics of resonant microbeam in vacuum", *Sensors and Actuators A*, **77** 191-194

Newell, W.E., 1967, "Miniaturization of Tuning Forks", *Science*, **161**(3848), p 1320-1326.

Schaaf, S.A., and Chambre, P.L., 1961, *Flow of Rarefied Gases*, Princeton University Press, NJ.

Sumali., H., Torczynski, J.R., Epp, D.S., and Gallis, M.A., 2007, "Experimental Validation of a Squeeze-Film Damping Model Based on Molecular Gas Dynamics", *Proc. 2007 ASME International Design Engineering Technical Conferences, September 4-7*, to appear.

Veijola, T., 2004, "Compact models for squeezed-film dampers with inertial and rarefied gas effects", *Journal of Micromechanics and Microengineering*, **14**, p 1109-1118.

Zook, J.D., Burns, D.W., Guckel, H., Sniegowski, J.J., Engelstad R.L., and Feng Z., 1992, "Characteristics of polysilicon resonant microbeams", *Sensors and Actuators A*, **35** 51-59.